Journal of Innovative Optical Health Sciences
Vol. 5, No. 4 (2012) 1250029 (7 pages)

DOI: 10.1142/S1793545812500290





# COLOR CORRECTION FOR HIGH-DEFINITION ELECTRONIC ENDOSCOPE

CHEN JING*, WANG LI-QIANG*, MENG ZI-BO*,
YUAN BO* and DUAN HUI-LONG†
*State Key Laboratory of Modern Optical Instrumentation
Zhejiang University, Hangzhou, Zhejiang 310027, P. R. China
†Biomedical Engineering Institute, Zhejiang University
Hangzhou, Zhejiang 310027, P. R. China

Accepted 12 August 2012
Published 1 October 2012

The subtle color distinction is the important function of electronic endoscope imaging diagnosis. However, after image acquisition, transmission and display, color distortions of intracorporeal organs or tissues occur inevitably, which are adverse to analyze image features accurately or to diagnose early pathological changes. A real-time color correction algorithm based on four-neighborhood and polynomial regression in *YUV* color space is proposed. Based on polynomial regression the color correction matrix is calculated in *YUV* color space according to the differences between standard values of color checker and measured values of that imaged by the endoscope. As the correction is only executed on *U* and *V* components in *YUV* color space, the defect that the color of corrected images in *RGB* color space will change along with luminance can be avoided, and then the stability of image color is improved. Owing to four-neighborhood processing, the signal-to-noise ratio of corrected images is enhanced and the processing speed of correction algorithm is accelerated. The average color difference is reduced from 0.3944 to 0.2850 by application of the proposed algorithm in high-definition electronic endoscope. A total of 17 frames per second can be achieved at the resolution of 1280 × 800, and the color characteristics of the image after processing match that of human visual system.

*Keywords*: High-definition electronic endoscope; color correction; polynomial regression; four-neighborhood.

## 1. Introduction

Medical electronic endoscopes have the advantages of user-friendly operating, intuitive and clear imaging, convenience of long-distance observation and control.[1] Important information and corresponding enhanced characteristics of the images can be obtained by further image processing technology, quantitative analysis and accurate diagnosis of the lesion can be realized. Medical electronic endoscopes have become one of the essential modern medical instruments.[2,3]

The diagnosis of the electronic endoscope images mainly depends on the subtle changes of the shape and color of the tissues such as vessels and mucous membranes. The color distortion of the electronic endoscope imaging of the actual diseased tissue will

happen inevitably after the exposure to the external light source, the image acquisition by the endoscope system and the display on a monitor.[4] Thus it will cause many adverse effects on the analysis of endoscopic images. On one hand, the doctors may make some wrong judgments when observing the endoscopic images, which will directly affect the diagnosis of the lesions and the doctor's acceptance of the endoscope. On the other hand, color distortion also affects the image feature extraction and subsequent image processing accuracy. Therefore, before image analysis, one of the key points of endoscopic image pre-processing is color correction,[5] which plays an important part in ensuring the veracity of the system and color characteristic suitable for human visual system.[6,7]

There are some common color correction methods such as methods based on grayscale,[8] restoring of spectral reflectance,[4] restoring of tristimulus values, the least square matrix and polynomial regression, respectively.[9] Color correction method based on grayscale can correct the image color and eliminate effects of exterior light to a certain extent,[8] but it is only suitable for the situation that does not require accurate effect of color correction.[10] The accuracy of the color correction method based on restoring of spectral reflectance on the basis of the finite-dimensional linear model is high, but the computation is too complex to meet the real-time applications.[4] The color correction method based on restoring of tristimulus values deduces the transformation matrix of $R$, $G$ and $B$ of images according to the equality of the tristimulus values before and after correction. The algorithm has some effect on color correction, while it also produces more image noise with poor color stability. The least square matrix fitting algorithm (LSMFA) aims to minimize the sum of squares of error between the standard values and testing imaging values in a particular lighting condition. The color correction effect of the algorithm is obvious, but the algorithm will produce larger image noise and reduce the endoscope system imaging smoothness and color stability. Polynomial regression method relies on the number of data fitting items which means that the regression accuracy improves along with increasing number of polynomial items. However, the color correction effect would not be better with more polynomial items which lead to degradation of image quality and losing of many details.[11]

To obtain more accurate, stable and smooth effect of color correction, a real-time color correction algorithm based on four-neighborhood polynomial regression in $YUV$ color space to correct endoscopic images is proposed in this paper.

## 2. Experimental Platform

The experimental platform of the whole endoscope system is shown in Fig. 1, which includes a light

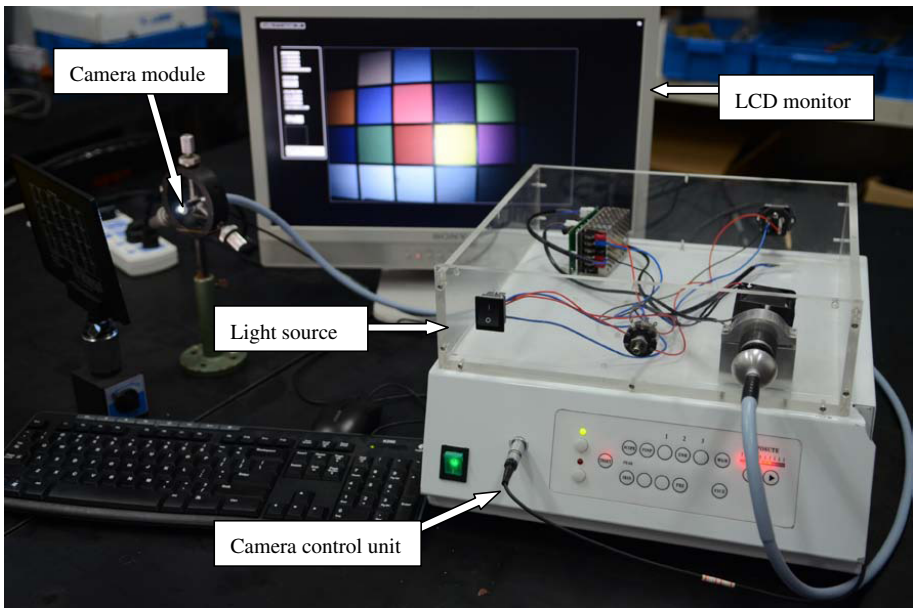


Fig. 1. Experiment system of high definition medical electronic endoscope system.

source (LUX2101-A1, FIAT LUX), a camera module (CAM1280-L1, FIAT LUX), a camera control unit (CCU7350-L1, FIAT LUX) and an LCD monitor (LMD-2110MC, SONY). The white light generated by the light source is directly coupled into an optical fiber bundle, and the end of the optical fiber bundle is integrated together with the camera module (laparoscope type). The camera module is connected by a custom cable to the camera control unit. The image processing workstation software is used for image display and processing. After the system is powered on, real-time video is displayed on the LCD monitor. During the course of video processing, the digital video or images can be captured and stored in the hard disk at any time.

One of the most important functions of the camera control unit is color correction during surgical guidance. A novel algorithm of color correction will be proposed and described on the following pages.

## 3. Algorithmic Model

It is shown in the previous studies that the colors corrected by LSMFA based on $RGB$ color space changes with illuminating brightness, which degrades the color stability and impacts endoscopic image processing and diagnosis. It is because LSMFA based on $RGB$ color space must deal with all of $R$, $G$ and $B$ components, which contain luminance information of images, to calculate the fitting matrix. Therefore $YUV$ color space is chosen for image correction to avoid the defect.

The importance of adopting $YUV$ color space is that luminance signal ($Y$) and chrominance signal ($U$ and $V$) are separated.[12] In the process of color correction based on $YUV$ color space, it is only necessary to deal with $U$ and $V$ components of image pixels, while original $Y$ components remain unchangeably, so the corrected image color does not change with luminance.

There are masses of image noises after image correction by LSMFA based on $RGB$ color space and color correction algorithm based on restoration of tristimulus values. To avoid a mass of image noises, four-neighborhood method is proposed rather than traditional point-by-point scanning. In the four-neighborhood method, four neighboring pixels of an original image are regarded as a processing unit,[13] and their coordinates are $(i, j)$, $(i, j+1)$, $(i+1, j)$ and $(i+1, j+1)$, where $i$ and $j$ stand for the row and column, respectively. Then the $RGB$ values of the four neighborhood pixels are transformed to $YUV$ values; and then the four $U$ and $V$ components are replaced by their averages, respectively, while the four $Y$ components remain unchanged. The processing method is reasonable because luminance is more sensitive to human eyes rather than chrominance.

It is testified in the experiment that the color cast of the corrected images is serious if only using $U$ and $V$ components in polynomial regression. Better correction effects of the hue and saturation are obtained with $U$, $V$ and $UV$ in polynomial regression. However, the corrected images using $U$, $V$, $UV$, $U^2$ and $V^2$ in polynomial regression with the loss of details and low processing speed cannot meet the real-time requirements of electronic endoscope. Therefore, the $U$, $V$ and $UV$ components are adopted for the polynomial regression calculation.

The correction coefficient matrix $A$ is figured out according to the measured values and the standard values of the color checker. Finally $U$ and $V$ components corrected by matrix $A$, together with original $Y$ components are transformed to new $R$, $G$ and $B$ values of four neighborhood pixels.

The key of color correction method based on four-neighborhood polynomial regression in $YUV$ color space is to establish correction model. Based on the analysis above, the correction model is shown in Fig. 2.

## 4. Concrete Realization

The correction matrix $A$ in Fig. 2 is determined by the polynomial regression using the testing $YUV$ values of the endoscopic imaging and the standard $YUV$ values of corresponding color checker. The distance between the color checker and the camera module is 150 mm, which is a typical working distance of laparoscope. Under this distance 24 color zones of Mennon color checker are measured by endoscope under the condition of the same illumination. Endoscopic image of each color zone is orderly displayed on the central area of LCD, where 50 pixels are chosen to calculate the mean values of $R$, $G$ and $B$ for each color zone by the software. According to the Eq. (1),[14] the $R$, $G$ and $B$ are transformed to $Y$, $U$ and $V$ values, while the

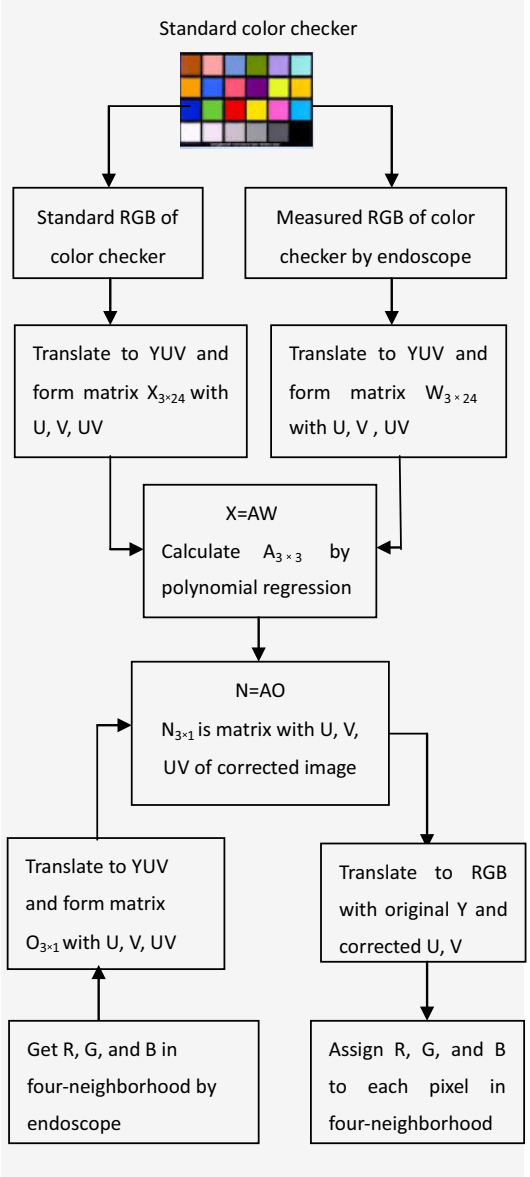


Fig. 2. Color correction model.

standard $R$, $G$ and $B$ of each color zone of the color checker are transformed into $YUV$ color space also, marked with $Y_O$, $U_O$ and $V_O$.

$$\begin{bmatrix} Y \\ U \\ V \end{bmatrix} = \begin{bmatrix} 0.299 & 0.587 & 0.114 \\ -0.1687 & -0.3313 & 0.5 \\ 0.5 & -0.418 & -0.082 \end{bmatrix} \bullet \begin{bmatrix} R \\ G \\ B \end{bmatrix} + \begin{bmatrix} 0 \\ 128 \\ 128 \end{bmatrix}. \quad (1)$$

Then according to polynomial regression, standard $U_O$, $V_O$ and $U_O V_O$ are calculated as Eq. (2) with the linear combination of measured $U$, $V$ and $UV$:

$$\begin{cases} U_O = a_{11}U + a_{12}V + a_{13}UV, \\ V_O = a_{21}U + a_{22}V + a_{23}UV, \\ U_O V_O = a_{31}U + a_{32}V + a_{33}UV. \end{cases} \quad (2)$$

The matrix form of Eq. (2) is shown as follows:

$$X = AW. \quad (3)$$

In Eq. (3), $X$ is a $3 \times 24$ matrix made up of standard $U$, $V$ and $UV$ of each color zone of the standard color checker:

$$X = \begin{bmatrix} U_{o1} & U_{o2} & \cdots & U_{o24} \\ V_{o1} & V_{o2} & \cdots & V_{o24} \\ UV_{o1} & UV_{o2} & \cdots & UV_{o24} \end{bmatrix}. \quad (4)$$

$W$ is also a $3 \times 24$ matrix, which is made up of measured $U$, $V$ and $UV$ of each color zone of the standard color checker:

$$W = \begin{bmatrix} U_{I1} & U_{I2} & \cdots & U_{I24} \\ V_{I1} & V_{I2} & \cdots & V_{I24} \\ UV_{I1} & UV_{I2} & \cdots & UV_{I24} \end{bmatrix}. \quad (5)$$

Matrix $A$ can be calculated based on the least square principle:

$$A = X \bullet W^T \bullet (W \bullet W^T)^{-1}. \quad (6)$$

The matrix $A$ is just the parameter of correction model, where superscript $T$ and $-1$ stand for the transposition and inverse of a matrix. Obviously the conversion coefficient matrix $A$ is a 3*3 one:

$$A = \begin{pmatrix} a_{11} & a_{12} & a_{13} \\ a_{21} & a_{22} & a_{23} \\ a_{31} & a_{32} & a_{33} \end{pmatrix}. \quad (7)$$

Finally $RGB$ values of each four pixels based on four-neighborhood method are figured out in each frame of measured endoscopic images, and then transformed to $YUV$ values as before. The $3 \times 1$ matrix $O$ made up of $U$, $V$ and $UV$ components is multiplied by conversion matrix $A$ to generate new $U$ and $V$ components. The new $U$ and $V$ together with the original $Y$ component are transformed to new $RGB$ values, as shown in Eq. (8)[14]:

$$\begin{bmatrix} R \\ G \\ B \end{bmatrix} = \begin{bmatrix} 1 & 0 & 1.402 \\ 1 & -0.344 & -0.714 \\ 1 & 1.772 & 0 \end{bmatrix} \bullet \begin{bmatrix} Y \\ U \\ V \end{bmatrix} + \begin{bmatrix} -179 \\ 135.4 \\ -227 \end{bmatrix}. \quad (8)$$

The actual $RGB$ values of each four-neighborhood pixels are determined by the new $RGB$ values, and then real-time color correction is achieved.

Each endoscope system has its own correction coefficient matrix which needs to test by the approach above. Then the algorithm is applied as a function of the corresponding camera control unit. The algorithm is easy to realize and the function is convenient to operate.

## 5. Experimental Results

The comparison of uncorrected image with corrected image based on four-neighborhood polynomial regression in $YUV$ color space are shown as Figs. 3 and 4, where the upper image is the uncorrected one obtained by the endoscope while the nether image is the corrected one.

As shown in Fig. 3, the color of the corrected image of color checker is very close to the true hue and saturation of the color checker, without obvious noise, with fine color stability and suitable for human visual characteristics.

As shown in Fig. 4, the contrast of the corrected endoscopic image of the oral cavity is enhanced comparing with the uncorrected image. The hue and saturation of the blood vessels and mucous membrane of the corrected image is more suitable for human visual characteristics which is beneficial to accurate diagnosis. The details of the corrected image is reserved well when the model of four-neighborhood is adopted.

Table 1 shows three types of values of six typical color zones of color checker: standard values uncorrected measured values and corrected values.

Table 2 shows the spatial chromatic aberration[15] between uncorrected measured $RGB$ values and corrected value of typical color zones of the color checker. The formula of calculating spatial chromatic aberration is shown in Eq. (9).[15]

$$\Delta rgb = \sqrt{(\Delta r)^2 + (\Delta g)^2 + (\Delta b)^2}/255. \quad (9)$$

The average chromatic aberration drops from 0.3944 before correction to 0.2850 after correction, referring to the standard $RGB$ values.

The main purpose of color correction is to improve the hue and saturation of images. Figure 5 shows the comparison between uncorrected and corrected hue and saturation of typical color zones of color checker, where polar angle and radius stand

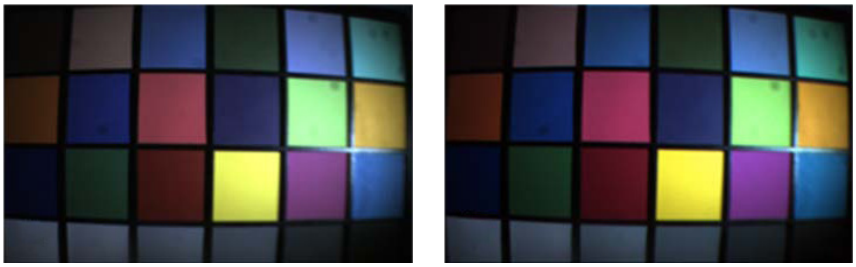

(a) (b)

Fig. 3. Comparison of uncorrected and corrected images of the color checker [(a) uncorrected image, (b) corrected image].

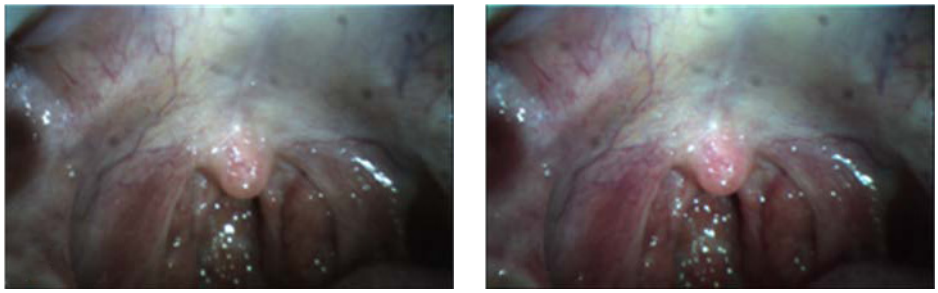

(a) (b)

Fig. 4. Comparison of uncorrected and corrected images of the oral cavity [(a) uncorrected image, (b) corrected image].

Table 1. Comparison of uncorrected and corrected colors.

| Test Colors | Standard Colors ($R$, $G$, $B$) | Uncorrected Colors ($R$, $G$, $B$) | Corrected Colors ($R$, $G$, $B$) |
|---|---|---|---|
| Blue | (44, 56, 142) | (46, 43, 56) | (31, 41, 102) |
| Green | (74, 148, 81) | (65, 100, 76) | (34, 120, 48) |
| Red | (179, 42, 50) | (223, 170, 128) | (255, 148, 103) |
| Yellow | (250, 226, 21) | (251, 255, 167) | (255, 255, 63) |
| Magenta | (191, 81, 160) | (172, 124, 136) | (200, 93, 213) |
| Cyan | (6, 142, 172) | (65, 87, 98) | (27, 100, 123) |

Table 2. Comparison of color differences.

| Test Colors | Uncorrected Color Difference | Corrected Color Difference |
|---|---|---|
| Blue | 0.3412 | 0.2853 |
| Green | 0.1925 | 0.3126 |
| Red | 0.6126 | 0.5194 |
| Yellow | 0.5837 | 0.1246 |
| Magenta | 0.2070 | 0.1077 |
| Cyan | 0.4293 | 0.3604 |
| Average error | 0.3944 | 0.2850 |

for hue and saturation, respectively. Compared with uncorrected values, both hue and saturation of corrected values are more close to the standard ones.

As shown in Fig. 6, images A, B, C and D are orderly the uncorrected endoscopic image of the green zone of color checker, the image corrected by LSMFA based on $RGB$ color space, the corrected image based on restoration of tristimulus values and the image corrected by the proposed method.

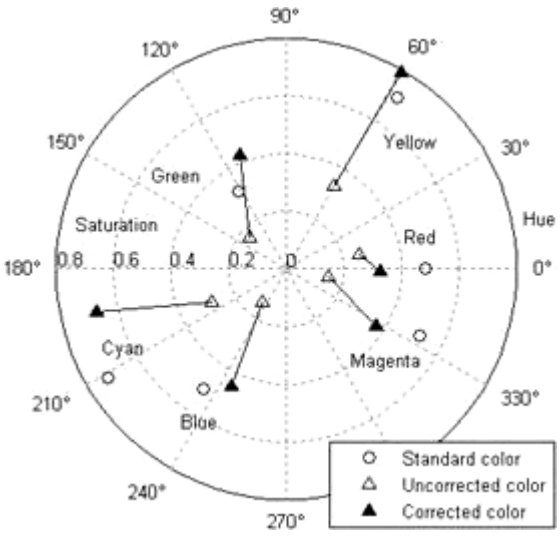


Fig. 5. Comparison of hue and saturation.

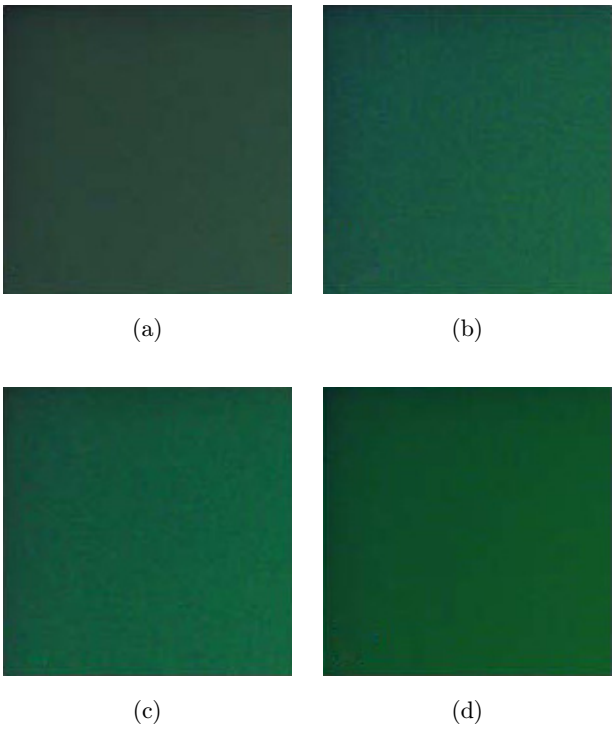


Fig. 6. Corrected images of different algorithm.

Obviously, either of the first two corrections generates masses of image noises, while the proposed correction algorithm improves the smoothness of images with few noises.

## 6. Conclusion

A new real-time high-definition electronic endoscopic images color correction algorithm is proposed in the paper. Compared with other color correction algorithms, high efficiency, accuracy and color stability of the proposed algorithm are highlighted. The experimental results show that the algorithm based on four-neighborhood polynomial regression in $YUV$ color space recovers the actual hue and saturation of the objects well. And the color of the

corrected images does not change with the brightness. The average chromatic aberration drops from 0.3944 before correction to 0.2850 after correction. The corrected images which has fine color stability and no noise pixels accord with human visual color characteristics. The frame rate of endoscope with high-definition resolution of 1280*800 is 17 frames per second by employing the proposed color correction and it meets the requirement of real-time image display, which provides the prerequisite for the accurate diagnosis and characteristic extracting of lesions. In addition, the proposed algorithm can also be used in the fields of other image color corrections, and has fine applicability.

## Acknowledgments

The work has been supported by grants from National Key Technology R&D Program (Grant No.: 2011BAI12B06) and the Fundamental Research Funds for the Central Universities (Grant No.: 2012FZA5023).

## References

1. S. Paul, A. Toor, F. Volke *et al.*, "Remote magnetic manipulation of a wireless capsule endoscope in the esophagus and stomach of humans," *Gastrointest. Endosc.* **71**(7), 1290−1293 (2010).
2. Z. Wang, L. Wang, S. Li, H. Jian, "Electronic endoscope insertion into a thoracic drainage tube is a new technique in the treatment and diagnosis of pleural diseases," *Surg. Endosc.* **23**(7), 1671−1673 (2009).
3. R. Mouri, S. Yoshida, S. Tanaka, S. Oka, M. Yoshihara, K. Chayama, "Evaluation and validation of computed virtual chromo endoscopy in early gastric cancer," *Gastrointest. Endosc.* **69**(6), 1052−1058 (2009).
4. H. Hideaki, T. Shiobara, Y. Miyake, "Color correction for colorimetric color reproduction in an electronic endoscope," *Opt. Commun.* **114**(1-2), 57−63 (1995).
5. Y. Cai, M. Cao, X. Zhang, L. Shen, "Finite dimension model based tongue color correction," *World Sci. Technol./Modernization of Traditional Chinese Medicine and Materia Medica* **9**(5), 116−121 (2007).
6. G. Li, W. Luo, P. Li, "Color image enhancement based on visual characteristics of human eyes," *Optoelectron. Eng.* **36**(11), 92−95 (2009).
7. Z. Chen, X. Wang, X. Zou, W. Jin, "A novel quality evaluation method for false color fused image based on human visual system," *Acta Photonica Sin.* **41**(4), 451−455 (2012).
8. X. Xu, Y. Cai, X. Liu, C. Liu, L. Shen, "Improved grey world color correction algorithms," *Acta Photonica Sin.* **39**(3), 559−564 (2010).
9. X. Xu, L. Shen, C. Liu, "Color correction methods and application in image processing," *Appl. Res. Comput.* **25**(8), 2250−2254 (2008).
10. Y. Wang, A. Wang, L. Shen, "A study of colour reproduction method of colour image," *China Illum. Eng. J.* **12**(2), 4−10 (2001).
11. X. Zhang, H. Xu, "Adaptively polynomial model based on Gaussian weighted function for colorimetric characterizaion of image devices," *Acta Opt. Sin.* **30**(s1), 100,415−100,419 (2010).
12. H. Xu, *Color Information Engineering*, Zhejiang University Press, Hangzhou (2006).
13. R. Zhao, *Digital Image Processing Introduction*, Northwestern Polytechnical University Press, Xi'an (1996).
14. D. Shao, J. Han, "Inter-transformation between YUV and RGB," *J. Changchun University* **14**(4), 51−53 (2004).
15. S. Dun, H. Wei, M. Sun, "A new distance color difference formula in RGB color space," *Sci. Technol. Engrg.* **11**(8), 1833−1836 (2011).